Biointerface Research in Applied Chemistry
Open-Access Journal (ISSN: 2069-5837)

Article
Volume 14, Issue 3, 2024, 60
https://doi.org/10.33263/BRIAC143.060

MHD Flow Past an Impulsively Started Inclined Plate with Parabolic Plate Velocity in the Presence of Thermal Diffusion and Thermal Radiation

Kalyan Chamuah [1,*], Nazibuddin Ahmed [2]

[1] Department of Mathematics, Gauhati University, Guwahati-781014, Assam, India; kalyanchamuah60@gmail.com (K.C.); saheel_nazib@yahoo.com (N.A.);
* Correspondence: kalyanchamuah60@gmail.com (K.C.);

Scopus Author ID 9636158600

Received: 25.06.2022; Accepted: 17.07.2022; Published: 4.02.2023

Abstract: An exact analysis of a radiative hydromagnetic flow behavior over a parabolic plate through a permeable medium along with variable species concentration and fluid temperature in the presence of a slated magnetic field parameter, chemical reaction, soret effect, radiation, and heat generation has been carried out closed-form analytical benchmark solutions for flow governing equations are obtained by using Laplace transform method. The effects of the parameters entering the problem on the flow and transport characteristics are studied graphically. It is observed that the velocity decreases with the increase of magnetic parameter, whereas it increases with the increasing value of Soret number, thermal Grashof number, and solutal Grashof number. Also, the magnitude of skin friction increases with accelerating parameters.

Keywords: MHD; parabolic inclined plate; chemical reaction; radiation; Soret number.

Nomenclature

$\vec{q}$ fluid velocity vector;
ρ fluid density, $\frac{kg}{m^3}$;
ν kinematic viscosity, $\frac{m^2}{s}$;
$\vec{J}$ current density vector;
$\vec{B}$ magnetic flux density vector;
$\vec{g}$ acceleration vector due to gravity;
κ thermal conductivity, $\frac{W}{m.K}$;
p fluid pressure;
K chemical reaction;
w dimensional velocity field;
w_o reference velocity;
b accelerating parameter;
b' dimensional accelerating parameter;
a^* heat absorption;
σ^* Stefan-Boltzmann constant;
D_M mass diffusivity, $\frac{m^2}{s}$;
D_T thermal diffusivity, $\frac{m^2 kmol}{K.s}$;
T' fluid temperature, K;
C' molar species concentration, $\frac{kmol}{m^3}$;
u dimensional fluid velocity;

t time;

C_S' species concentration at the plate;

q_r radiative heat flux;

C_p specific heat at constant pressure, $\frac{Joule}{kg \times K}$

σ electrical conductivity, $\frac{1}{(ohm.m)}$;

$\vec{E}$ electrical field;

β , coefficient of thermal expression, $\frac{1}{k}$;

β^* coefficient of solutal expansion, $\frac{1}{kmol}$;

Q heat source;

Q' dimensional heat source;

K chemical reaction;

B_o strength of the applied magnetic field, Tesla;

γ inclination angle of the plate;

k_p' dimensional permeability;

T_∞' undisturbed temperature, K;

φ angle of inclination of magnetic field;

k_p permeability;

C_∞' free stream species concentration, kmol/m^3;

w' plate velocity;

T_S' fluid temperature at the plate;

N radiation parameter;

μ coefficient of viscosity, $\frac{kg}{ms}$;

θ dimensionless temperature;

ϕ dimensionless concentration;

Pr Prandtl number;

Sc Schmidt number;

Sr Soret number;

Gr thermal Grashof number;

Gm solutal Grashof number;

M magnetic parameter;

1. Introduction

MHD, also known as Magneto-Fluid Dynamics, is concerned with studying the interaction of magnetic fields and electrically conducting fluids in motion in the presence of the magnetic field. Numerous examples of applying MHD principles are found in our natural life systems. Dynamo and motor are considered to be classic examples of the MHD principle. Applications of MHD principles are widely seen in the case of fusion reactors, the design of MHD pumps, MHD generators, MHD flow meters, etc. The principles of MHD are also utilized in medical and biological sciences. Alfven [1], Shercliff [2], Cowling [3], Ferraro and Plumpton [4], and Crammer and Pai [5] are some notable authors whose contributions lead MHD to the present form.

A material containing voids or pore spaces, free of solid, embedded in the solid or semi-solid matrix is a porous material. Its permeability mainly characterizes it to a variety of fluids. That is, fluids can penetrate through one face of a material sample and emerge on the other side. Therefore, the porous material is encountered everywhere in day-to-day activities in nature and technology. Many different technologies, such as hydrology and petroleum engineering, depend on porous material. Due to this reason, fluid flows in porous media have gained the great attention of many scholars. A model for boundary conditions of a porous material under the issues of viscous fluid flow past a porous solid has been investigated by Taylor [6] and Richardson [7]. Moreover, the following researchers, Chen *et al*. [8], Chavent and Jaffri [9], Endalew and Sarkar [10], and Ahmed and Bordoloi [11], are widely devoted to the investigations of transport through porous media.

When heat and mass transfer coincide in a moving fluid, the relations connecting the fluxes and driving potentials are more intricate. It is seen that a mass flux can be generated not only by composition gradient but by temperature gradient as well. The effect concerned with the mass flux under temperature gradient is the Soret effect. Renowned Chemist Charles Soret first performed the experimental investigation of this effect in 1879, and so this effect is known as the Soret effect in honor of his name. The Soret effect is concerned with separating heavier gas molecules from lighter ones by ramped temperature gradient over a given volume of a gas containing particles of different manners. The Soret effect is also termed the thermal diffusion effect. Roughly speaking, the thermal diffusion effect deals with the mass flux resulting from the temperature difference. A comprehensive literature on various aspects of thermal diffusion on different kinds of mass transfer-related problems can be found in Eckert and Drake [12], Kafousias and Williams [13], Nandi and Kumbhakar [14], Ahmed and Sarma [15], Kalyan and Ahmed [16], Singh *et al*. [17], Illias *et al*. [18], and Ahmed *et al*. [19]. Recently Ahmed [20] has obtained an exact solution to the problem of MHD-free convective mass transfer flow of an incompressible viscous electrically conducting non-gray optically thin fluid past an impulsively started semi-infinite vertical plate with ramped wall temperature in the presence of thermal radiation, thermal diffusion, and under the imposition of a uniform transverse magnetic field.

None of the studies mentioned above incorporate radiation, which can play a vital role in industrial and space technology applications. Physically speaking, thermal radiation is an energy emission as subatomic particles in motion, especially particles with a high amount of energy that can cause ionization. The infrared radiation emitted by a typical household radiator or electric heater can be considered a typical thermal radiation example. Analytical investigation of the effects of thermal radiation parameters on time-dependent hydromagnetic flow over an inclined linearly moving plate through a permeable medium has been discussed by Endalew and Nayak [21]. The influence of thermal radiation parameters on a non-Newtonian fluid flow through a porous medium was investigated by Sobamowo *et al*. [22].

An inclined magnetic field is an additional consideration of equivalent utility, particularly for industrial applications and biological examinations. The variation of the inclination angle of this magnetic field is between 0 and 90 degrees. The influence of an inclined magnetic field on time-dependent hydromagnetic flow over an inclined oscillatory plate and linearly accelerating plate is discussed by Endalew *et al*. [23] and Endalew and Nayak [24]. An inclined magnetic field on the time-dependent squeezing flow between parallel plates with suction/injection is discussed by Su and Yin [25].

MHD flow problems dealing with the motion caused by suddenly starting infinitely long vertical plates with parabolic (non-linear) velocity have been studied by many researchers due to their possible applications in astrophysics, geophysics, missile technology, etc. Some of them are Muthucumarswamy and Sivakumar [26], Rajaiah *et al*. [27], and Agarwalla and Ahmed [28]. Most recently, Endalewand and Sarkar [29] performed an exact analysis of the problem, which deals with incidences of a tilted magnetic field on a transit radiative hydromagnetic flow over a slanted parabolic accelerated plate through a porous material with the occurrence of the chemical reaction and heat-generating parameter.

The study of the effect of chemical reactions on heat and mass transfer in a flow is of great practical importance to Engineers and Scientists because of its almost universal occurrence in many branches of science and technology. Heat and mass transfer occur simultaneously in many processes, such as drying, energy transfer in a wet cooling tower, and

flow in a desert cooler. Possible applications of these types of flow problems are found in many industries. Many researchers have studied the effect of chemical reactions on different convective heat and mass transfer flows, of whom Ramakrishna *et al*. [30], Devi *et al*. [31], Hazarika and Ahmed [32], Gurram *et al*. [33], Megaraju and Shekar [34], Choudhury *et al*. [35], and Shera *et al*. [36], are worth mentioning. Reddy and Reddy [37] investigated the problem dealing with the effects of viscous dissipation on free convection MHD flow through a porous medium across an exponentially stretching surface in the presence of a chemical reaction. Usharani and Selvaraj [38] investigated the influence of an MHD stream passing through an exponentially inclined vertical plate of first-order chemical reaction with variable mass diffusion and thermal radiation.

As per the author's knowledge, no attempt has been made to date to investigate the problem of free convective MHD flow of a viscous incompressible electrically conducting non-Gray optically thick chemically reactive and radiating fluid past an impulsively started semi-infinite vertical plate with parabolic plate velocity, temperature, and concentration in the presence of thermal radiation taking into account the thermal diffusion effect. However, such an attempt has been made in the present work.

2. Materials and Methods

2.1. Basic equations.

Equation of continuity:

$$\vec{\nabla}.\vec{q} = 0 \tag{1}$$

Magnetic field continuity equation:

$$\vec{\nabla}.\vec{B} = 0 \tag{2}$$

Ohm's law for moving conductor:

$$\vec{J} = \sigma\left(\vec{E} + \vec{q} \times \vec{B}\right) \tag{3}$$

MHD momentum equation with buoyancy force:

$$\rho\left[\frac{\partial \vec{q}}{\partial t'} + \left(\vec{q}.\vec{\nabla}\right)\vec{q}\right] = -\vec{\nabla}p + \vec{J} \times \vec{B} + \rho\vec{g} + \mu\nabla^2\vec{q} - \frac{\mu\vec{q}}{k_p} \tag{4}$$

Energy equation:

$$\rho C_P\left[\frac{\partial T'}{\partial t'} + \left(\vec{q}.\vec{\nabla}\right)T'\right] = \kappa\nabla^2 T' - \vec{\nabla}.q_r + Q\left(T' - T'_\infty\right) \tag{5}$$

Species continuity equation:

$$\frac{\partial C'}{\partial t'} + \left(\vec{q}.\vec{\nabla}\right)C' = D_M\nabla^2 C' - K'\left(C' - C'_\infty\right) + D_T\nabla^2 T' \tag{6}$$

Equation of state according to classical Boussinesq approximation:

$$\rho_\infty = \rho\left[1+\beta\left(T'-T'_\infty\right)+\beta^*\left(C'-C'_\infty\right)\right] \qquad (7)$$

All the physical quantities are defined in the Nomenclature.

2.2. Mathematical formulation.

Consider the one-dimensional unsteady hydromagnetic flow of electrically conducting, incompressible, heat-generating, as well as chemically reacting fluid over an inclined parabolic accelerated plate within the porous medium. A rectangular Cartesian Co-ordinate system is so chosen that x' and y' -axes to be in vertical and horizontal directions. A constant magnetic field B_o is applied at an arbitrary angle ϕ with the x' axis so that the magnetic field vector influencing the flow is given $B = (B_o \cos\varphi,\ B_o \sin\varphi,\ 0)$. In addition, the plate is supposed to be slanted by an arbitrary angle γ . At the initial time, $\left(t'=0\right)$ the plate is stationary. However $t'>0$, the plate starts to move in its own plane parabolically with velocity $w = w_o\left(b't'^2\right)$. In Figure 1, the geometry of the problem is clearly demonstrated. In order to make the mathematical model idealized, the present theoretical investigation is carried out under the following assumptions:

I. All the fluid properties, excluding the density in the buoyancy force term, are constants.
II. The Magnetic Reynolds number is too small to ignore the induced magnetic field.
III. Viscous and Ohmic dissipations of energy are negligible.
IV. No external electric field is applied to the system.
V. The plate is an electrical insulator.
VI. Both inclinations are supposed to be in the vertical direction.
VII. Levels of both temperature and concentration are changed linearly with time.

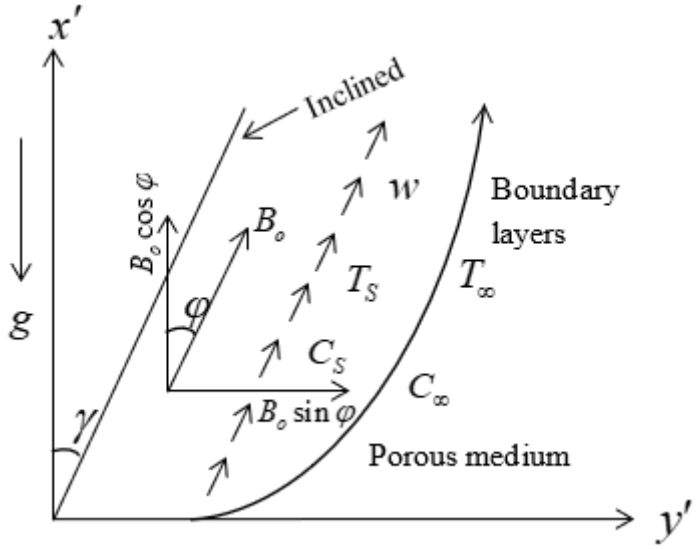

Figure 1. Physical configuration.

The above assumption leads to the governing equations of motion in terms of mass continuity, momentum, energy, and species continuity, which are as follows:

$$\frac{\partial w}{\partial x'} = 0 \qquad (8)$$

$$\frac{\partial w}{\partial t'}=\nu\frac{\partial^2 w}{\partial y'^2}-\left(\frac{\sigma B_o^2\sin^2\varphi}{\rho}+\frac{\nu}{k_p'}\right)w+(\cos\gamma)g\beta^*(C'-C_\infty')+(\cos\gamma)g\beta(T'-T_\infty') \tag{9}$$

$$\rho C_P\frac{\partial T'}{\partial t'}=-\frac{\partial q_r}{\partial y'}+\kappa\frac{\partial^2 T'}{\partial y'^2}+Q'(T'-T_\infty') \tag{10}$$

$$\frac{\partial C'}{\partial t'}=D_M\frac{\partial^2 C'}{\partial y'^2}+D_T\frac{\partial^2 T'}{\partial y'^2}-K'(C'-C_\infty') \tag{11}$$

Subject to initial and boundary conditions

$$\left.\begin{aligned} t'\le 0: w=0,\ C'=C_\infty',\ T'=T_\infty' \quad for\ all\ y'\\ t'>0: w=w_o\left(b't'^2\right),\\ (T'-T_\infty')\nu=(T_S'-T_\infty')w_o^2t',\\ (C'-C_\infty')\nu=(C_S'-C_\infty')w_o^2t',\ at\ y'=0,\\ w'\to 0,\ C'\to C_\infty',\ T'\to T_\infty'\ at\ y'\to\infty. \end{aligned}\right\} \tag{12}$$

Here, considered an optically thin gray gas, then we have (England and Emery [39]) the following mathematical expression:

$$\frac{\partial q_r}{\partial y'}=-4a^*\sigma^*\left(T_\infty'^4-T'^4\right) \tag{13}$$

Noting the fact that $|T'-T_\infty'|$ is very small, T'^4 may be expanded as follows

$$T'^4=\left(T'-T_\infty'+T_\infty'\right)^4=\left\{T_\infty'+(T'-T_\infty')\right\}=4T'T_\infty'^3-3T_\infty'^4 \tag{14}$$

By using Equations (13) and (14), in (10) we have

$$\rho C_P\frac{\partial T'}{\partial t'}=\kappa\frac{\partial^2 T'}{\partial y'^2}-16a^*\sigma^*T_\infty'^3(T'-T_\infty')+Q'(T'-T_\infty') \tag{15}$$

Now, to make the mathematical model of the problem normalized, the following group of non-dimensional quantities is introduced

$$\left.\begin{aligned} &y=\frac{y'w_o}{\nu},\ t=\frac{t'w_o^2}{\nu},\ u=\frac{w}{w_o},\ Gr=\frac{\nu g\beta(T_S'-T_\infty')}{w_o^3},\\ &Gm=\frac{\nu g\beta^*(C_S'-C_\infty')}{w_o^3},\ \theta=\frac{T'-T_\infty'}{T_S'-T_\infty'},\ b=\frac{b'\nu^2}{w_o^4},\ \mathrm{Pr}=\frac{\mu C_P}{\kappa}\\ &\phi=\frac{C'-C_\infty'}{C_S'-C_\infty'},\ k_p=\frac{k_p'w_o^2}{\nu^2},\ K=\frac{K'\nu}{w_o^2},\ M=\frac{\sigma B_o^2\nu}{\rho w_o^2},\\ &N=\frac{16a^*\sigma^*T_\infty'^3\nu}{\rho C_P w_o^2},Q=\frac{\nu Q'}{\rho C_P w_o^2},Sc=\frac{\nu}{D_M},Sr=\frac{D_T(T_S'-T_\infty')}{\nu(C_S'-C_\infty')} \end{aligned}\right\} \tag{16}$$

So, Equations (9), (11), and (15) are transformed into the non-dimensional form are as follows:

$$\frac{\partial u}{\partial t}=\nu\frac{\partial^2 u}{\partial y^2}-\left(M\sin^2\varphi+\frac{1}{k_P}\right)u+\left(\cos\gamma\right)Gr\theta+\left(\cos\gamma\right)Gm\phi \tag{17}$$

$$\Pr\frac{\partial\theta}{\partial t}=\frac{\partial^2\theta}{\partial y^2}-(N-Q\Pr)\theta \tag{18}$$

$$\frac{\partial\phi}{\partial t}=\frac{1}{Sc}\frac{\partial^2\phi}{\partial y^2}+Sr\frac{\partial^2\theta}{\partial y^2}-K\phi \tag{19}$$

The initial and boundary conditions in the non-dimensional form are

$$\left.\begin{array}{l} t=0: u=0,\ \phi=0,\ \theta=0\ \ for\ all\ \ y \\ t>0: u=bt^2,\ \ \theta=t,\ \ \phi=t, at\ y=0 \\ u\to 0,\ \theta\to 0,\ \ \phi\to 0\ \ as\ \ y\to\infty \end{array}\right\} \tag{20}$$

2.3 Method of solution.

On taking Laplace Transforms of Equations (17)-(19) and condition (20), the combined initial and the boundary value problem gets reduced to a pure boundary value problem governed by the following linear ordinary differential equations:

$$\frac{d^2\bar{u}}{dy^2}-(s+\lambda)\bar{u}+Gr\,\bar{\theta}\cos\gamma+Gm\bar{\phi}\cos\gamma=0 \tag{21}$$

$$\frac{d^2\bar{\theta}}{dy^2}-\left(\delta+s\Pr\right)\bar{\theta}=0 \tag{22}$$

$$\frac{d^2\bar{\phi}}{dy^2}-Sc\left(K+s\right)\bar{\phi}+Sc\,Sr\frac{d^2\theta}{dy^2}=0 \tag{23}$$

where $\lambda=M\sin^2\varphi+\dfrac{1}{k_p}$ and $\delta=N-Q\Pr$

Subject to the conditions:

$$\left.\begin{array}{l} \bar{u}=\dfrac{b}{s^3},\ \bar{\theta}=\dfrac{1}{s^2},\ \bar{\phi}=\dfrac{1}{s^2}\ at\ \ y=0 \\ \bar{u}\to 0,\ \bar{\theta}\to 0,\ \ \bar{\phi}\to 0\ \ as\ \ y\to\infty \end{array}\right\} \tag{24}$$

The equations (21) - (23) are solved subject to the condition (24) and the solutions are as follows:

$$\bar{\theta}=\frac{e^{-y\sqrt{s\Pr+\delta}}}{s^2} \tag{25}$$

$$\bar{\phi} = \frac{1}{s^2} e^{-y\sqrt{Sc(s+K)}} + \lambda_1 \left[\frac{e^{-y\sqrt{Sc(s+k)}} - e^{-y\sqrt{s\,\mathrm{Pr}+\delta}}}{s^2(s-\alpha_1)} \right] \tag{26}$$

$$\bar{u} = \frac{b}{s^3} e^{-y\sqrt{s+\lambda}} + \lambda_2 \left[\frac{e^{-y\sqrt{s\,\mathrm{Pr}+\delta}} - e^{-y\sqrt{s+\lambda}}}{s^2(s-\alpha_2)} \right] + \lambda_3 \left[\frac{e^{-y\sqrt{Sc(s+K)}} - e^{-y\sqrt{s+\lambda}}}{s^2(s-\alpha_3)} \right] + \lambda_5 \left[\frac{e^{-y\sqrt{Sc(s+K)}} - e^{-y\sqrt{s+\lambda}}}{s^2(s-\alpha_1)(s-\alpha_3)} \right] + \lambda_6 \left[\frac{e^{-y\sqrt{s+\lambda}} - e^{-y\sqrt{s\,\mathrm{Pr}+\delta}}}{s^2(s-\alpha_1)(s-\alpha_2)} \right] \tag{27}$$

where, $\alpha_1 = \dfrac{ScK-\delta}{\mathrm{Pr}-Sc}$, $\alpha_2 = \dfrac{\delta-\lambda}{1-\mathrm{Pr}}$, $\alpha_3 = \dfrac{ScK-\lambda}{1-Sc}$

$\lambda_1 = \dfrac{ScSr(s\,\mathrm{Pr}+\delta)}{(\mathrm{Pr}-Sc)}$, $\lambda_2 = \dfrac{Gr\cos\gamma}{(1-\mathrm{Pr})}$, $\lambda_3 = \dfrac{Gc\cos\gamma}{(1-Sc)}$,

$\lambda_4 = \dfrac{Gc\cos\gamma}{(1-\mathrm{Pr})}$, $\lambda_5 = \lambda_1\lambda_3$, $\lambda_6 = \lambda_1\lambda_4$

Taking inverse Laplace Transforms of the solutions (25) – (27), the expressions for non-dimensional temperature θ , concentration ϕ , and velocity field u are in the following forms:

$$\theta = f\left(\mathrm{Pr}, \frac{\delta}{\mathrm{Pr}}, y, t\right) \tag{28}$$

$$\phi = f(Sc, K, y, t) + \lambda_1 \left[\begin{array}{l} \dfrac{1}{\alpha_1^2} e^{\alpha_1 t} \left\{ \psi(Sc, \alpha_1 + K, y, t) - \psi\left(\mathrm{Pr}, \alpha_1 + \dfrac{\delta}{\mathrm{Pr}}, y, t\right) \right\} - \\ \dfrac{1}{\alpha_1} \left\{ f(Sc, K, y, t) - f\left(\mathrm{Pr}, \dfrac{\delta}{\mathrm{Pr}}, y, t\right) \right\} - \\ \dfrac{1}{\alpha_1^2} \left\{ \psi(Sc, K, y, t) - \psi\left(\mathrm{Pr}, \dfrac{\delta}{\mathrm{Pr}}, y, t\right) \right\} \end{array} \right] \tag{29}$$

$$u = b\Lambda_1(\eta,\lambda,t) + \lambda_2\alpha_{12}\left[\psi\left(\Pr,\frac{\delta}{\Pr},y,t\right) - h(\lambda,y,t)\right] + \lambda_2\alpha_{13}\left[f\left(\Pr,\frac{\delta}{\Pr},y,t\right) - \Lambda_2(\eta,\lambda,t)\right] - \lambda_2\alpha_{12}e^{\alpha_2 t}\left[\psi\left(\Pr,\alpha_2+\frac{\delta}{\Pr},y,t\right) - h(\alpha_2+\lambda,y,t)\right] + \lambda_3\alpha_{14}\left[\psi(Sc,K,y,t) - h(\lambda,y,t)\right] + \lambda_3\alpha_{15}\left[f(Sc,K,y,t) - \Lambda_2(\eta,\lambda,t)\right] - \lambda_3\alpha_{14}e^{\alpha_3 t}\left[\psi(Sc,K+\alpha_3,y,t) - h(\alpha_3+\lambda,y,t)\right] + \lambda_5\alpha_7\left[\psi(Sc,K,y,t) - h(\lambda,y,t)\right] + \alpha_4\lambda_5\left[f(Sc,K,y,t) - \Lambda_2(\eta,\lambda,t)\right] + \lambda_5\alpha_5 e^{\alpha_1 t}\left[\psi(Sc,\alpha_1+K,y,t) - h(\alpha_1+\lambda,y,t)\right] + \lambda_5\alpha_6 e^{\alpha_3 t}\left[\psi(Sc,\alpha_3+K,y,t) - h(\alpha_3+\lambda,y,t)\right] + \lambda_6\alpha_8\left[h(\lambda,y,t) - \psi\left(\Pr,\frac{\delta}{\Pr},y,t\right)\right] + \lambda_6\alpha_9\left[\Lambda_2(\eta,\lambda,t) - f\left(\Pr,\frac{\delta}{\Pr},y,t\right)\right] + \lambda_6\alpha_{10}e^{\alpha_1 t}\left[h(\alpha_1+\lambda,y,t) - \psi\left(\Pr,\alpha_1+\frac{\delta}{\Pr},y,t\right)\right] + \lambda_6\alpha_{11}e^{\alpha_2 t}\left[h(\alpha_2+\lambda,y,t) - \psi\left(\Pr,\alpha_2+\frac{\delta}{\Pr},y,t\right)\right] \quad (30)$$

where $\eta = \frac{y}{2\sqrt{t}}$, $\alpha_4 = \frac{1}{\alpha_1\alpha_3}$, $\alpha_5 = \frac{1}{\alpha_1^2(\alpha_1-\alpha_3)}$,

$\alpha_6 = \frac{1}{\alpha_3^2(\alpha_3-\alpha_1)}$, $\alpha_7 = -\alpha_5 - \alpha_6$, $\alpha_8 = -\alpha_{10} - \alpha_{11}$,

$\alpha_9 = \frac{1}{\alpha_1\alpha_2}$, $\alpha_{10} = \frac{1}{\alpha_1^2(\alpha_1-\alpha_2)}$, $\alpha_{11} = \frac{1}{\alpha_2^2(\alpha_2-\alpha_1)}$,

$\alpha_{12} = -\frac{1}{\alpha_2^2}$, $\alpha_{13} = -\frac{1}{\alpha_2}$, $\alpha_{14} = -\frac{1}{\alpha_3^2}$, $\alpha_{15} = -\frac{1}{\alpha_3}$,

$\phi_1(\eta,\lambda,t) = e^{2\eta\sqrt{\lambda t}}erfc\left(\eta+\sqrt{\lambda t}\right) + e^{-2\eta\sqrt{\lambda t}}erfc\left(\eta-\sqrt{\lambda t}\right)$,

$\bar{\phi}_1(\eta,\lambda,t) = e^{2\eta\sqrt{\lambda t}}erfc\left(\eta+\sqrt{\lambda t}\right) - e^{-2\eta\sqrt{\lambda t}}erfc\left(\eta-\sqrt{\lambda t}\right)$,

$\Lambda_1(\eta,\lambda,t) = \frac{(\eta^2+\lambda t)t}{4\lambda}\phi_1(\eta,\lambda,t) - \frac{\eta\sqrt{t}(1-4\lambda t)}{8\lambda^{3/2}}\bar{\phi}_1(\eta,\lambda,t) - \frac{\eta t}{2\lambda\sqrt{\pi}}e^{-(\eta^2+\lambda t)}$,

$\Lambda_2(\eta,\lambda,t) = \frac{1}{2}\left\{\left(t+\eta\sqrt{\frac{t}{\lambda}}\right)e^{2\eta\sqrt{\lambda t}}erfc\left(\eta+\sqrt{\lambda t}\right) + \left(t-\eta\sqrt{\frac{t}{\lambda}}\right)e^{-2\eta\sqrt{\lambda t}}erfc\left(\eta-\sqrt{\lambda t}\right)\right\}$,

$f(Sc,K,y,t) = \left(\frac{t}{2}+\frac{y}{4}\sqrt{\frac{Sc}{K}}\right)e^{\sqrt{ScK}y}erfc\left(\frac{y}{2}\sqrt{\frac{Sc}{t}}+\sqrt{Kt}\right) + \left(\frac{t}{2}-\frac{y}{4}\sqrt{\frac{Sc}{K}}\right)e^{-\sqrt{ScK}y}erfc\left(\frac{y}{2}\sqrt{\frac{Sc}{t}}-\sqrt{Kt}\right)$

$h(\lambda,y,t) = \frac{1}{2}\left[e^{2\eta\sqrt{\lambda t}}erfc\left(\eta+\sqrt{\lambda t}\right) + e^{-2\eta\sqrt{\lambda t}}erfc\left(\eta-\sqrt{\lambda t}\right)\right]$,

$$\psi\left(Sc,K,y,t\right)=\frac{1}{2}\left[e^{\sqrt{ScK}y}erfc\left(\frac{y}{2}\sqrt{\frac{Sc}{t}}+\sqrt{Kt}\right)+e^{-\sqrt{ScK}y}erfc\left(\frac{y}{2}\sqrt{\frac{Sc}{t}}-\sqrt{Kt}\right)\right],$$

2.4 Coefficient of the rate of momentum transfer.

The viscous drag per unit area on the plate in the direction of the plate velocity, based on Newton's law of viscosity velocity, is as follows:

$$\bar{\tau}=-\mu\frac{\partial u'}{\partial y'}\Bigg]_{y'=0}$$

The coefficient of skin friction or the coefficient of the rate of momentum transfer at the plate is given by

$$\tau=-\frac{\partial u}{\partial y}\Bigg]_{y=0}$$

$$=-\left[\begin{array}{l}
b\Lambda_{1y}^{o}\left(\eta,\lambda,t\right)+\lambda_2\alpha_{12}\left\{\psi_y^o\left(\Pr,\frac{\delta}{\Pr},y,t\right)-h_y^o\left(\lambda,y,t\right)\right\}+\lambda_2\alpha_{13}\left\{f_y^o\left(\Pr,\frac{\delta}{\Pr},y,t\right)-\Lambda_{2y}^{o}\left(\eta,\lambda,t\right)\right\}\\
-\lambda_2\alpha_{12}e^{\alpha_2 t}\left\{\psi_y^o\left(\Pr,\alpha_2+\frac{\delta}{\Pr},y,t\right)-h_y^o\left(\alpha_2+\lambda,y,t\right)\right\}+\lambda_3\alpha_{14}\left\{\psi_y^o\left(Sc,K,y,t\right)-h_y^o\left(\lambda,y,t\right)\right\}+\\
\lambda_3\alpha_{15}\left\{f_y^o\left(Sc,K,y,t\right)-\Lambda_{2y}^{o}\left(\eta,\lambda,t\right)\right\}-\lambda_3\alpha_{14}e^{\alpha_3 t}\left\{\psi_y^o\left(Sc,K+\alpha_3,y,t\right)-h_y^o\left(\alpha_3+\lambda,y,t\right)\right\}+\\
+\lambda_5\alpha_7\left\{\psi_y^o\left(Sc,K,y,t\right)-h_y^o\left(\lambda,y,t\right)\right\}+\alpha_4\lambda_5\left\{f_y^o\left(Sc,K,y,t\right)-\Lambda_{2y}^{o}\left(\eta,\lambda,t\right)\right\}+\lambda_5\alpha_5e^{\alpha_1 t}\\
\left\{\psi_y^o\left(Sc,\alpha_1+K,y,t\right)-h_y^o\left(\alpha_1+\lambda,y,t\right)\right\}+\lambda_5\alpha_6e^{\alpha_3 t}\left\{\psi_y^o\left(Sc,K+\alpha_3,y,t\right)-h_y^o\left(\alpha_3+\lambda,y,t\right)\right\}+\\
\lambda_6\alpha_8\left\{h_y^o\left(\lambda,y,t\right)-\psi_y^o\left(\Pr,\frac{\delta}{\Pr},y,t\right)\right\}+\lambda_6\alpha_9\left\{\Lambda_{2y}^{o}\left(\eta,\lambda,t\right)-f_y^o\left(\Pr,\frac{\delta}{\Pr},y,t\right)\right\}+\lambda_6\alpha_{10}e^{\alpha_1 t}\\
\left\{h_y^o\left(\alpha_1+\lambda,y,t\right)-\psi_y^o\left(\Pr,\alpha_1+\frac{\delta}{\Pr},y,t\right)\right\}+\lambda_6\alpha_{11}e^{\alpha_2 t}\left\{h_y^o\left(\alpha_2+\lambda,y,t\right)-\psi_y^o\left(\Pr,\alpha_2+\frac{\delta}{\Pr},y,t\right)\right\}
\end{array}\right] \quad (31)$$

where

$$\phi_{1y}^{o}=-2\sqrt{\lambda}erf\left(\sqrt{\lambda t}\right)-\frac{2e^{-\lambda t}}{\sqrt{\pi t}},$$

$$\bar{\phi}_{1y}^{o}=-2erf\left(\sqrt{\lambda t}\right)$$

$$\Lambda_{1y}^{o}\left(\eta,\lambda,t\right)=\frac{\lambda t^2}{4\lambda}\phi_{1y}^{o}-\bar{\phi}_{1y}^{o}\frac{\left(1-4\lambda t\right)}{16\lambda^{3/2}}-\frac{\sqrt{t}}{4\lambda\sqrt{\pi}}e^{-\lambda t},$$

$$\psi_y^o\left(Sc,K,y,t\right)=-\left[\sqrt{\frac{Sc}{\pi t}}e^{-Kt}+\sqrt{ScK}erf\left(\sqrt{Kt}\right)\right],$$

$$h_y^o\left(\lambda,y,t\right)=-\sqrt{\lambda}erf\left(\sqrt{\lambda t}\right)-\frac{e^{-\lambda t}}{\sqrt{\pi t}},$$

$$f_y^o\left(Sc,K,y,t\right)=-\left[\sqrt{\frac{Sc}{4K}}erf\left(\sqrt{Kt}\right)+t\sqrt{ScK}erf\left(\sqrt{Kt}\right)+\sqrt{\frac{tSc}{\pi}}e^{-Kt}\right],$$

$$\Lambda_{2y}^o\left(\eta,\lambda,t\right)=-\frac{erf\left(\sqrt{\lambda t}\right)}{2\sqrt{\lambda}}-t\sqrt{\lambda}erf\left(\sqrt{\lambda t}\right)-\sqrt{\frac{t}{\pi}}e^{-\lambda t}$$

2.5 Coefficient of the rate of mass transfer.

The mass flux M_w at the plate $y'=0$, determined by Fick's law of diffusion, is given by $M_w=-D_M\left.\frac{\partial C}{\partial y'}\right]_{y'=0}$

Thus, the coefficient of the rate of mass transfer at the plate in terms of Sherwood number is given by

$$Sh=-\left.\frac{\partial\phi}{\partial y}\right]_{y=0}$$

$$=-f_y^o\left(Sc,K,y,t\right)-\frac{\lambda}{\alpha_1^2}\left[\begin{array}{l}e^{\alpha_1 t}\left\{\psi_y^o\left(Sc,\alpha_1+K,y,t\right)-\psi_y^o\left(\Pr,\alpha_1+\frac{\delta}{\Pr},y,t\right)\right\}\\-\alpha_1\left\{f_y^o\left(Sc,K,y,t\right)-f_y^o\left(\Pr,\frac{\delta}{\Pr},y,t\right)\right\}\\-\left\{\psi_y^o\left(Sc,K,y,t\right)-\psi_y^o\left(\Pr,\frac{\delta}{\Pr},y,t\right)\right\}\end{array}\right] \quad (32)$$

2.6 Coefficient of the rate of heat transfer.

The heat flux $q*$ from the plate $y'=0$ to the fluid specified by the Fourier law of conduction is given by

$$q^*=-\bar{\kappa}\left.\frac{\partial T'}{\partial y'}\right]_{y'=0} \qquad ;\bar{\kappa}=\kappa+\frac{16\sigma^*T_\infty^3}{3\kappa^*}$$

The coefficient of the rate of heat transfer at the plate in terms of Nusselt number Nu is expressed as

$$Nu=-\left.\frac{\partial\theta}{\partial y}\right]_{y=0}$$

$$=\frac{\Pr}{2\sqrt{\delta}}erf\left(\sqrt{\frac{t\delta}{\Pr}}\right)+t\sqrt{\delta}erf\left(\sqrt{\frac{t\delta}{\Pr}}\right)+\sqrt{\frac{\Pr t}{\pi}}e^{-\frac{t\delta}{\Pr}} \quad (33)$$

3. Results and Discussion

In order to assess the physical situation of the theoretical problem, numerical computations for the velocity field u, temperature field θ, concentration field ϕ, skin friction τ, Nusselt number Nu, and the Sherwood number Sh are performed by assigning some specific values to the physical parameters, viz. thermal Grashof number Gr, solutal Grashof number Gm, chemical reaction K, thermal radiation N, Prandtl number Pr, Schmidt number Sc, heat source Q, magnetic parameter M, Soret number Sr, the permeability of the medium kp, plate inclination angle γ, angle of inclination of the magnetic field φ, accelerating parameter b and time t. The calculated results are represented graphically in Figures 2 to 16.

The variations in the velocity field u against y under the influence of magnetic parameter M, Soret number Sr, thermal Grashof number Gr, and solutal Grashof number Gm are displayed through graphs in terms of Figures 2-5. It is evident from Figure 2 that the fluid velocity decreases comprehensively for increasing magnetic parameter M. In other words, the fluid motion is decelerated due to the imposition of the transverse magnetic field. This observation is consistent with the physical fact that a magnetic body force develops due to the interaction of fluid velocity and magnetic field, which serves as a resistive force to the flow. Consequently, the fluid flow gets decelerated. It is observed from Figures 3, 4, and 5 that fluid velocity increases with the increase of Soret number Sr, thermal Grashof number Gr, and solutal Grashof number Gm. Thermal buoyancy force (Figure 4) and solutal buoyancy force (Figure 5) cause the velocity field to rise substantially. This is happening due to the direct proportionality of buoyancy force to those of Grashof numbers.

Figures 6-8 exhibit the variation temperature distribution θ versus y under the influence of thermal radiation N, Prandtl number Pr, and heat source Q. A clear fall in fluid temperature under the radiation effect is reflected in Figure 6. This phenomenon is in good agreement with the physical fact that thermal radiation always has a tendency to minimize the atmosphere's temperature. It is inferred from Figure 7 that an increase in Prandtl parameter Pr causes the fluid temperature to fall gradually. Prandtl number is described as a quotient of kinematic viscosity to thermal diffusivity. More precisely, it has an inverse proportionality with thermal diffusivity. Therefore, the larger Prandtl number generates the smaller thermal diffusivity. Hence, as the Prandtl number increases, the fluid temperature reduces due to the reduction of thermal diffusivity. A significant rise in temperature profile under the heat source Q effect is noticed in Figure 8. Heat source or heat-generating parameter Q yields the mechanism generating or producing thermal energy from the surrounding itself. It is more pronounced that more heat generation from its ambiances yields a high spread of fluid temperature. Therefore, when the heat-generating parameter increases, the fluid temperature also increases.

The effect of the Schmidt number Sc and chemical reaction K on the concentration profile are presented in Figures 9 and 10. A clear hike in concentration under Sc is reflected in Figure 9. It is noted that an increase in Sc means a fall in mass diffusivity. Thus, the concentration at the plate gets enhanced for low mass diffusivity. There is a significant rise in fluid concentration level under the effect of chemical reaction, which is visualized in Figure 10. This observation agrees with the physical reality that the consumption of species leads to a rise in species concentration.

The variation in skin friction τ against t under the influence of inclination angle γ and accelerating parameter b is displayed in Figures 11 and 12. From Figure 11, we can see that the coefficient of the rate of momentum transfer or viscous drag reduces with the increment of

an inclination angle γ of the plate, while a reverse trend is observed in Figure 12 with the increase in the value of accelerating parameter b.

The change of behavior of the coefficient of the mass transfer rate versus t under the influence of heat source Q and Soret number Sr is illustrated in Figures 13 and 14. These figures show that the Sherwood number increases with the effects of Q and Sr.

Figures 15 and 16 depict how the behavior of the coefficient of the rate of heat transfer changes with the variation of the values of the physical parameters thermal radiation N and heat source Q. It is observed from these figures that Nusselt number Nu rises due to the N effect, but falls under Q effect.

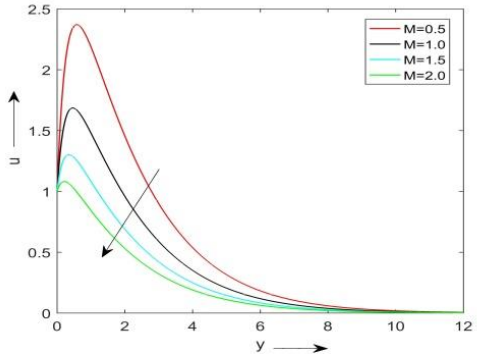

Figure 2. Velocity u versus y for $Gr = 1$, $Gm = 1$, $K = 2$, $N = 5$, $\Pr = .7$, $Sc = .6$, $Q = 5$, $kp = .5$, $\gamma = \pi/3$, $\varphi = \pi/3$, $Sr = 2$, $b = 1$ $t = 1$,

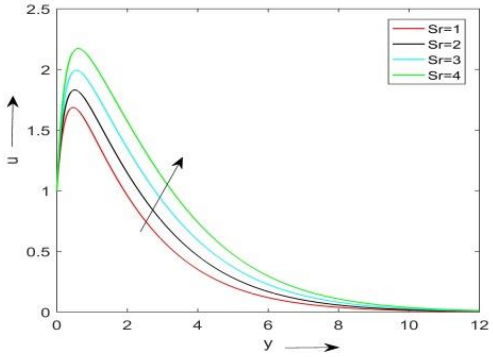

Figure 3. Velocity u versus y for $Gr = 1$, $Gm = 1$, $K = 2$, $N = 5$, $\Pr = .7$, $Sc = .6$, $Q = 5$, $M = 1$, $kp = .5$, $\gamma = \pi/3$, $\varphi = \pi/3$, $b = 1$ $t = 1$,

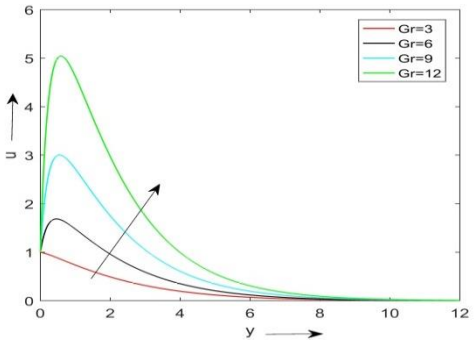

Figure 4. Velocity u versus y for $Gm = 1$, $K = 2$, $N = 5$, $\Pr = .7$, $Sc = .6$, $Q = 5$, $M = 1$, $kp = .5$, $\gamma = \pi/3$, $\varphi = \pi/3$, $Sr = 2$, $b = 1$, $t = 1$,

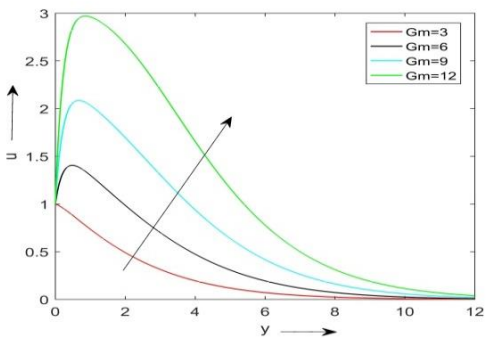

Figure 5. Velocity u versus y for $Gr = 1$, $K = 2$, $N = 5$, $\Pr = .7$, $Sc = .6$, $Q = 5$, $M = 1$, $kp = .5$, $\gamma = \pi/3$, $\varphi = \pi/3$, $Sr = 2$, $b = 1$, $t = 1$,

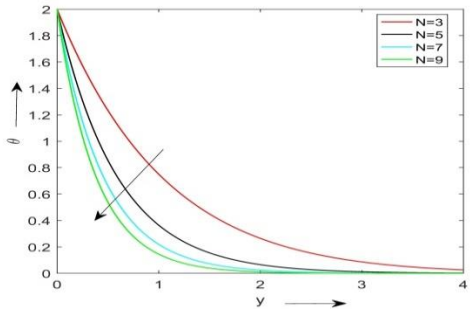

Figure 6. Temperature θ versus y for $\Pr = .7$, $Q = .5$, $t = 1$

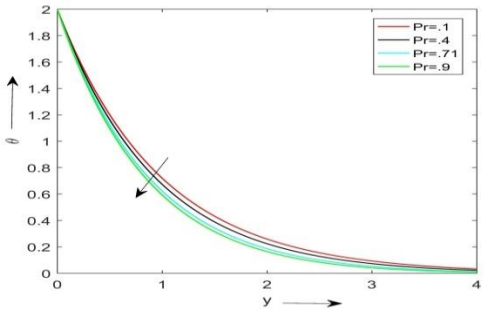

Figure 7. Temperature θ versus y for $N = 5$, $Q = .5$, $t = 1$

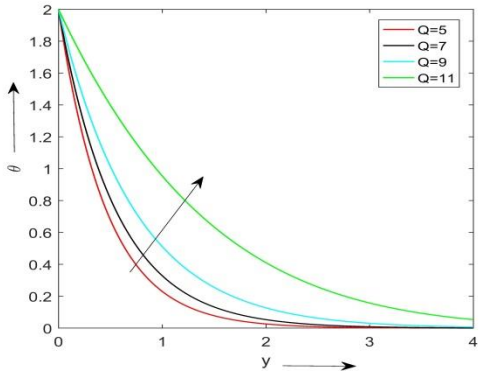

Figure 8. Temperature θ versus y for $\Pr = .7$, $N = 5$, $t = 1$

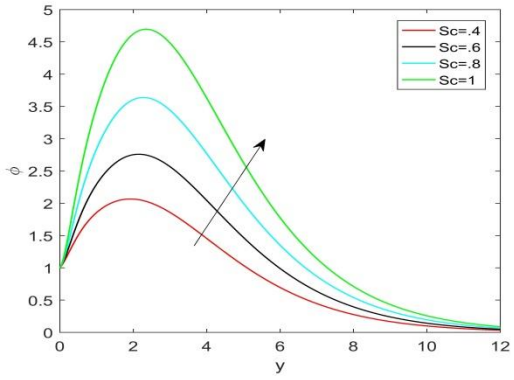

Figure 9. Concentration ϕ versus y for $K = .3$, $\Pr = .7$, $Sr = 2$, $\gamma = \pi/3$, $\varphi = \pi/3$, $N = 5$, $M = 1$, $Q = .5$, $t = 1$

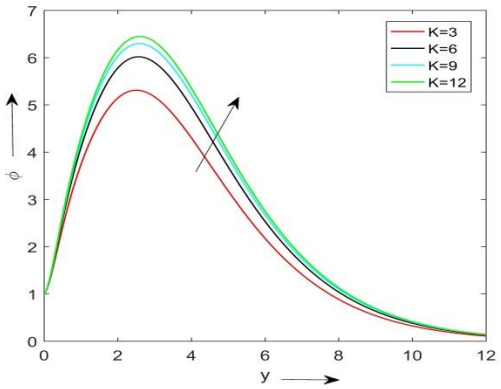

Figure 10. Concentration ϕ versus y for φ , $Sr = 2$, $Sc = .2$, $\gamma = \pi/3$, $\varphi = \pi/3$, $N = 5$, $M = 1$, $N = 5$, $M = 1$

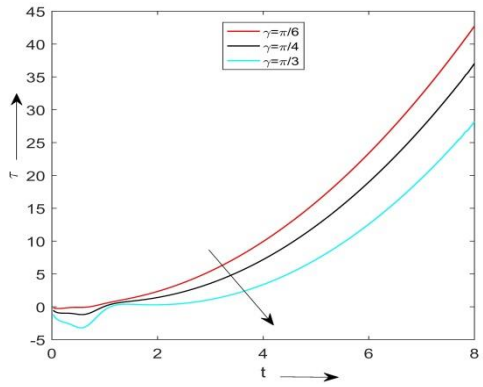

Figure 11. Skin friction τ versus t for $Gr = 1$, $Gm = 1$, $K = .1$, $N = 6$, $\Pr = .7$, $Sc = .6$, $Q = .5$, $M = 1$, $kp = .5$, $\varphi = \pi/3$, $Sr = 2$, $b = 1$

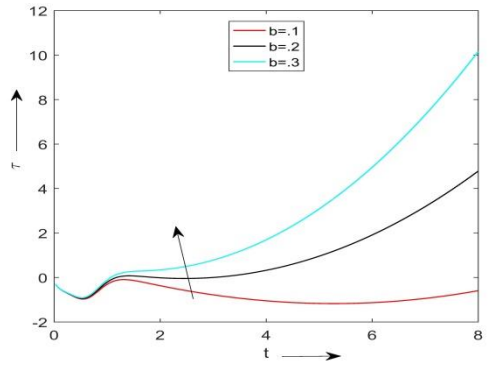

Figure 12. Skin friction τ versus t for $Gr = 1$, $Gm = 1$, τ , $N = 6$, $\Pr = .7$, $Sc = .6$, $Q = .5$, $M = 1$, $kp = .5$, $\gamma = \pi/3$, $\varphi = \pi/3$, $Sr = 2$

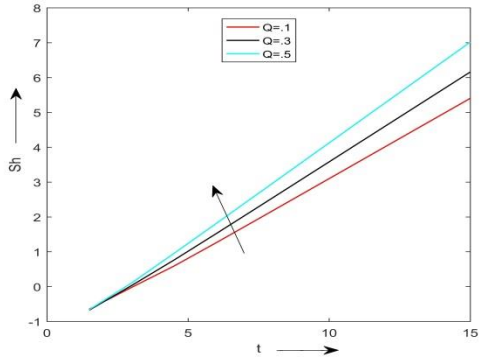

Figure 13. Sherwood number Sh versus t for $N = 1$, $\Pr = .7$, $Sc = .2$, $K = 1$, $Sr = 5$

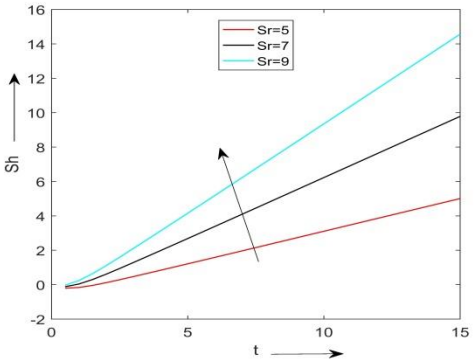

Figure 14. Sherwood number Sh versus t for $N = 1$, $Q = .6$, $\Pr = .7$, $Sc = .2$, $K = 1$

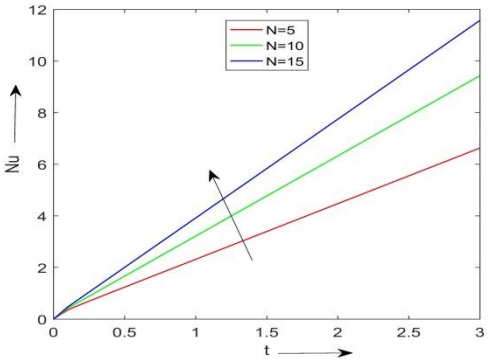

Figure 15. Nusselt number Nu versus t for $Q = .5$, $\Pr = .7$

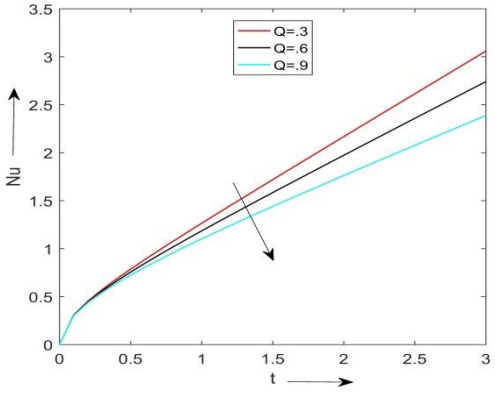

Figure 16. Nusselt number Nu versus t for $N = 5$, $\Pr = .7$

4. Conclusions

This paper analyzes the fluid flow problem over a tilted parabolic plate through a porous material with the occurrence of thermal radiation, Soret number and inclination of the magnetic field, and variable velocity, temperature, concentration, and transport properties investigated. Finally, the outcomes of the present investigation are: (i) The fluid velocity increases with the

increment of Soret number and buoyancy forces, reducing the magnetic parameter; (ii) The temperature reduces as Prandtl number and thermal radiation increase with the increase of heat source; (iii) Schmidt number and chemical reaction effects have significant contributions in raising the concentration level of the plate; (iv) The viscous drag increases with the accelerating parameter, whereas the increment in the plate inclination angle causes its reduction; (v) Rate of heat transfer or Nusselt number boosts when thermal radiation increases whereas it decreases with an increment in heat-generating parameter; (vi) Rate of mass transfer at the surface of the plate becomes high as Soret number and heat source become high.

Funding

This research received no external funding.

Acknowledgments

The authors would like to thank the anonymous reviewers for their valuable comments and suggestions to improve the paper's quality.

Conflicts of Interest

The authors declare no conflict of interest.

References

1. Alfven, H. Existence of electromagnetic-hydrodynamic wave. *Nature* **1942**, *150*, 405-406, https://doi.org/10.1038/150405d0.
2. Shercliff, J.A. A Text Book of Magnetohydrodynamics, London, Pergamon Press, **1965**.
3. Cowling T.G. Magnetohydrodynamics, New York, Wiley Inter Science, **1957**.
4. Ferraro, V.C.A.; Plumpton, C. An Introduction to Magneto-Fluid Mechanics. *Geophysical journal International* **1967**, *12*, 543-544, https://doi.org/10.1093/gji/12.5.543-a.
5. Crammer, K.R.; Pai, S.I. Magneto Fluid Dynamics for Engineers and Applied Physicist. New York, Mc Graw Hill Book Co. **1973**.
6. Taylor, G. A model for the boundary condition of a porous material, Part 1. *Journal of Fluid Mechanics* **1971**, *49*, 319-326, https://doi.org/10.1017/S0022112071002088.
7. Richardson, S. A model for the boundary condition of a porous material Part 2. *Journal of Fluid Mechanics* **1971**, *49*, 327-336, https://doi.org/10.1017/S002211207100209X.
8. Chen, Z.; Huan, G.; Ma, Y. Computational methods for multiphase flows in porous media. Vol. 2, Siam **2006,** http://doi.org/10.1137/1.9780898718942.
9. Chavent, G.; Jaffre, J. Mathematical models and finite elements for reservoir simulation, single phase, multiphase and multicomponent flows through porous media. *Elsevier*, **1986**.
10. Endalew, M.F.; Sarkar, S. Capturing the Transient Features of Double Diffusive Thin Film Flow of a Second Grade Fluid Through a Porous Medium. *International Journal of Applied and Computational Mathematics* **2019**, *5*, 160, https://doi.org/10.1007/s40819-019-0743-7.
11. Ahmed, N. and Bordoloi, R. Three-dimensional flow past a porous vertical plate in a porous medium with sinusoidal suction and permeability in the presence of thermal diffusion. *Heat Transfer* **2021**, https://doi.org/10.1002/htj.22325.
12. Eckert E.R.G.; Drake, R.M. Analysis of Heat and Mass Transfer. New York, Mc Graw-Hill Book Co. **1972**.
13. Kafoussias N.G.; Williams, E.W. Thermal diffusion and diffusion thermo effects on mixed free forced convective and mass transfer boundary layer flow with temperature dependent viscosity. *Int. J. Eng. Sci.* **1998**, *33*, 1369-1384, https://doi.org/10.1016/0020-7225(94)00132-4.
14. Nandi, S. and Kumbhakar, B. Hall current and thermo-diffusion effects on magnetohydrodynamics convective flow near an oscillatory plate with ramped type thermal and solutal boundary conditions. *Indian J. Phys.* **2021**, 1-14, https://doi.org/10.1007/S12648-020-02001-0.

15. Ahmed, N. and Sarma, S. Thermal diffusion effect on unsteady MHD free convective flow past an impulsively started but temporarily accelerated semi-infinite vertical plate with parabolic ramped conditions. *Heat transfer* **2021**, 1-33, https://doi.org/10.1002/htj.22295.
16. Chamuah, K.; Ahmed N. MHD free convective dissipative flow past a porous plate in a porous medium in the presence of radiation and thermal diffusion effects. *Heat Transfer* **2021**, https://doi.org/10.1002/htj.22383.
17. Singh, J.K., Seth, G.S., and Savanur, V.: Impacts of the periodic wall conditions to the hydromagnetic convective flow of viscoelastic fluid through a vertical channel with Hall current and induced magnetic field. *Heat transfer* **2021**, *50*, 1812-1835, https://doi.org/10.1002/htj.21957.
18. Ilias, M.R.; Ismail, N.S.; Ab Raji, N.H.; Rawi, N.A.; Shafie, S. Unsteady aligned MHD boundary layer flow and heat transfer of a magnetic nanofluids past an inclined plate. *Int. J. of Mech. Eng. and Robotics Research* **2020**, *9*, 197-206, https://doi.org/10.18178/ijmerr.9.2.
19. Ahmed, N.; Choudhury K. and Chamuah K. Three dimensional hydromagnetic convective flow past a porous vertical plate with sinusoidal suction in slip flow regime. *Mathematics in Engineering, Science and Aerospace* **2021**, *11*, 805-825.
20. Ahmed, N. MHD mass transfer flow past an impulsively started semi-infinite vertical plate with Soret effect and ramped wall temperature, In Smith, F.T., Dutta, H., Mardeson, J.N. (eds.), Mathematics Applied to engineering, Modelling, and Social Issues, Studies in system, Decision and Control **2019**, *200*, 245-279, https://doi.org/10.1007/978-3-030-12232-4_8.
21. Endalew, M.F.; Nayak, A. Thermal radiation and inclined magnetic field effects on MHD flow past a linearly accelerated inclined plate in a porous medium with variable temperature. *Heat Transfer Asian Research* **2019**, *48*, 42-61, https://doi.org/10.1002/HTJ.21367.
22. Sobamowo, M.; Yinusa, A.; Makinde, A. A study on the Effects of Inclined Magnetic Field Flow Medium Porosity and Thermal Radiation on Free convection of casson Nanofluid over a vertical plate. *World Scientific News* **2019**, *138*, 1-64.
23. Endalew, M.F.; Nayak, A.; Sarkar, S. Flow past an oscillating slanted plate under the effects of inclined magnetic field, radiation, chemical reaction and time varying temperature and concentration. *International Journal of Fluid Mechanics Research* **2020**, *47*, 247-261, https://doi.org/10.1615/interjfluidmechres.2020026987.
24. Endalew, M.F.; Nayak, A. Thermal radiation and inclined magnetic field effects on MHD flow past a linearly accelerated inclined plate in a porous medium with variable temperature. *Heat Transfer Asian Research* **2019**, *48*, 42-61, https://doi.org/10.1002/HTJ.21367.
25. Su, X.; Yin, Y. Effects of an inclined magnetic field on the unsteady squeezing flow between parallel plates with suction/injection. *Journal of Magnetism and Magnetic Materials* **2019**, *484*, 266-271, https://doi.org/10.1016/j.jmmm.2019.04.041.
26. Muthucumarswamy, R.; Sivakumar, P. MHD flow past a parabolic flow past an infinite isothermal vertical plate in presence of thermal radiation and chemical reaction. *Int. J. Appl. Mech. Eng.* **2016**, *21*, 95-105, https://doi.org/10.1515/ijame-2016-0006.
27. Rajaiah, M.; Sudhakaraiah, A.; Venkatalakshmi, P. Radiation and Soret effects on unsteady MHD flow past a parabolic started vertical plate in presence of chemical reaction with magnetic dissipation through a porous medium. *Int. J. Sci. Res.* **2015**, *4*, 1608-1613.
28. Agarwalla, S.; Ahmed, N. MHD mass transfer flow past an inclined plate with variable temperature and plate velocity embedded in a porous medium. *Heat transfer Asian Research* **2018**, *47*, 27-41, https://doi.org/10.1002/htj.21288.
29. Endalew, M.F.; Sarkar, S. Incidences of aligned magnetic field on unsteady MHD flow past a parabolic accelerated inclined plate in a porous medium. *Heat Transfer* **2021**, https://doi.org/10.1002/htj.22153.
30. Ramakrishna, S.B.; Thavada, S.K.; Venkatachala, G.M.; Bandaru, M. Impacts of Chemical Reaction, Diffusion-Thermo and Radiation on Unsteady Natural Convective Flow past an Inclined Vertical Plate under Aligned Magnetic Field. *Biointerface research in applied chemistry* **2021**, *11*, 13252-13267, https://doi.org/10.33263/BRIAC115.1325213267.
31. Devi, G.L.; Niranjan, H.; Sivasankaran, S. Effects of chemical reaction, radiation and activation energy effects on MHD buoyancy induced nanofluid flow past a vertical surface. *Interntional Journal of Science and Technology* **2021**, https://doi.org/10.24200/SCI.2021.56835.4934.

32. Hazarika, N.J. and Ahmed, S.: Thermo-diffusive flow of chemically reacting fluids in a saturated porous medium for radiative heat flux. *Journal of Scientific Research* **2021**, *13*, 507-520, https://doi.org/10.3329/JSR.V13I2.50425.
33. Gurram, D.; Balamurugan, K.S.; Raju, V.C.C.; Vedavathi, N. Effect of chemical reaction on magnetohydrodynamics casson fluid flow past an inclined surface with radiation. *Skit Res. J.* **2017**, *7*, 53-59.
34. Megaraju, P.; Shekar, M.N.R. Transient MHD flows through flows through an exponentially accelerated isothermal vertical plate with Hall effect and chemical reaction effect. *Partial differential equations in applied Mathematics* **2021**, *4*, https://doi.org/10.1016/j.padiff.2021.100047.
35. Choudhury, K; Ahmed, N; Chamuah, K. Radiation Effect on MHD Flow past a Porous Vertical Plate in the Presence of Heat Sink. *Heat transfer* **2022**, https://doi.org/10.1002/htj.22548.
36. Sehra; Haq, SU; Shah, SIA; Nisar, KS; Jan, SU and Khan, I. Convection heat mass transfer and MHD flow over a vertical plate with chemical reaction, arbitrary shear stress and exponential heating. *Scientific reports* **2021**, *11*, https://doi.org/10.1038/s41598-021-81615-8.
37. Reddy, N.N.; Reddy, B.R. Chemical reaction impact on MHD natural convection flow through porous medium past an exponentially stretching sheet in presence of heat source/sink and viscous dissipation. *Case studies in thermal engineering* **2021**, *25*, 100879, https://doi.org/10.1016/j.csite.2021.100879.
38. Usharani, V.; Selvaraj, A.; Constance Angela, R.; Neel Armstrong, A. Impact of magnetohydrodynamics stream past an exponentially inclined vertical plate of first order chemical response with variable mass diffusion with variable mass diffusion and thermal radiation. *Mathematical modelling and computational Science* **2021**, *1292*, 485-497, https://doi.org/10.1007/978-981-33-4389-4_45.
39. England, W.; Emery, A. Thermal radiation effects on the laminar free convection boundary layer of an absorbing gas. *Journal of Heat transfer* **1969**, *91*, 37-44, https://doi.org/10.1115/1.3580116.